Mass transfer models for sand ripples

1. Vortex ripples and wind ripples
2. Wavelength selection for vortex ripples
3. Stochastic coarsening of wind ripples

K.H. Andersen, M. Abel, J.K., C. Ellegaard, L.R. Søndergaard J. Udesen: PRL **88**, 234302 (2002)

E.K.O. Hellén, J.K.: PRE **66**, 011304 (2002)

J.K.: Adv. Complex Syst. **4**, 353 (2001)

EXPERIMENTAL SETUP

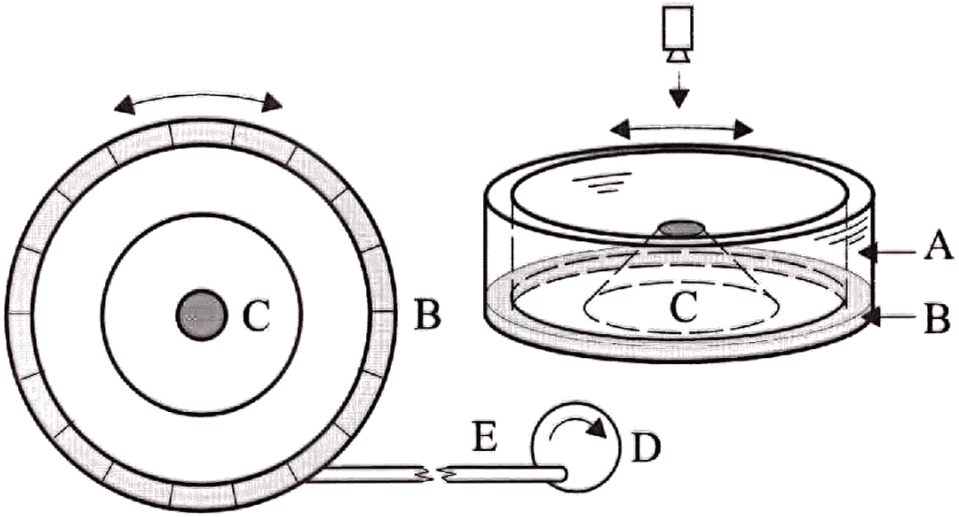

C. Ellegaard, L.R. Søndergaard, J. Udesen, NBI

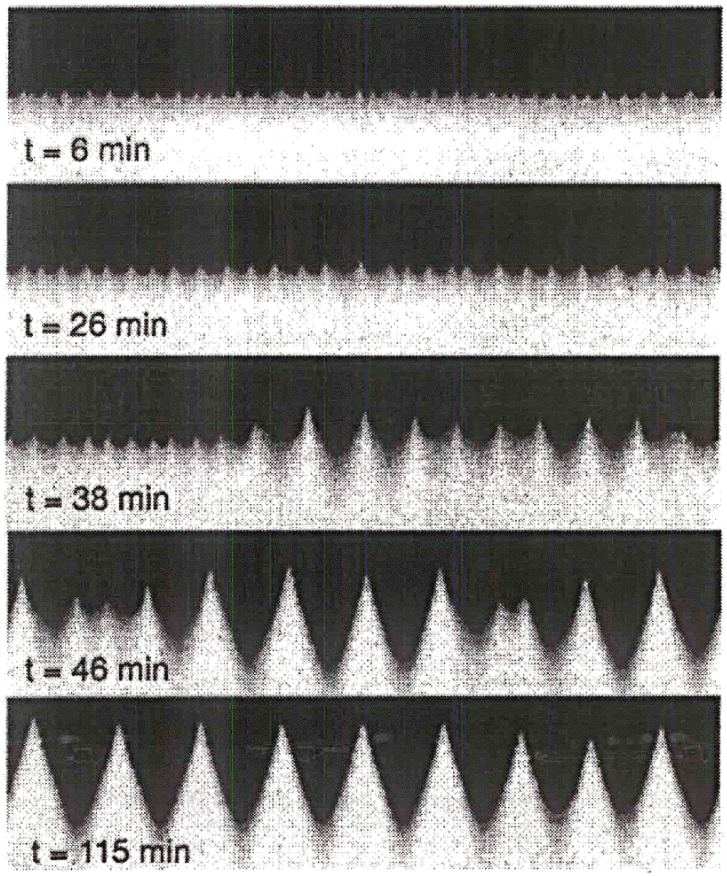

A. Stegner, J.E. Wesfreid, PRE 60, R 3487 (1999)

$\lambda = \frac{2}{3} \cdot L = \frac{4}{3} \cdot a$

a: oscillation amplitude

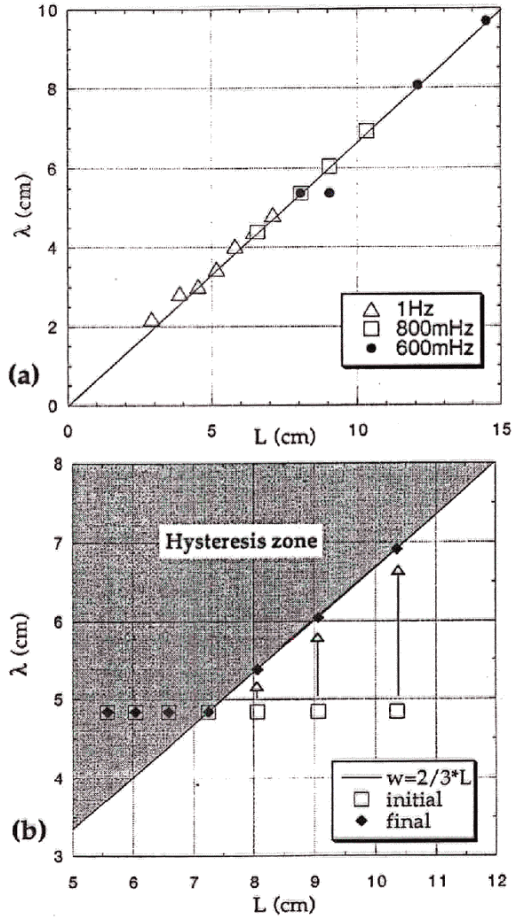

A. Stegner, J.E. Wesfreid, PRE 60, R 3487 (1999)

Phase diagram

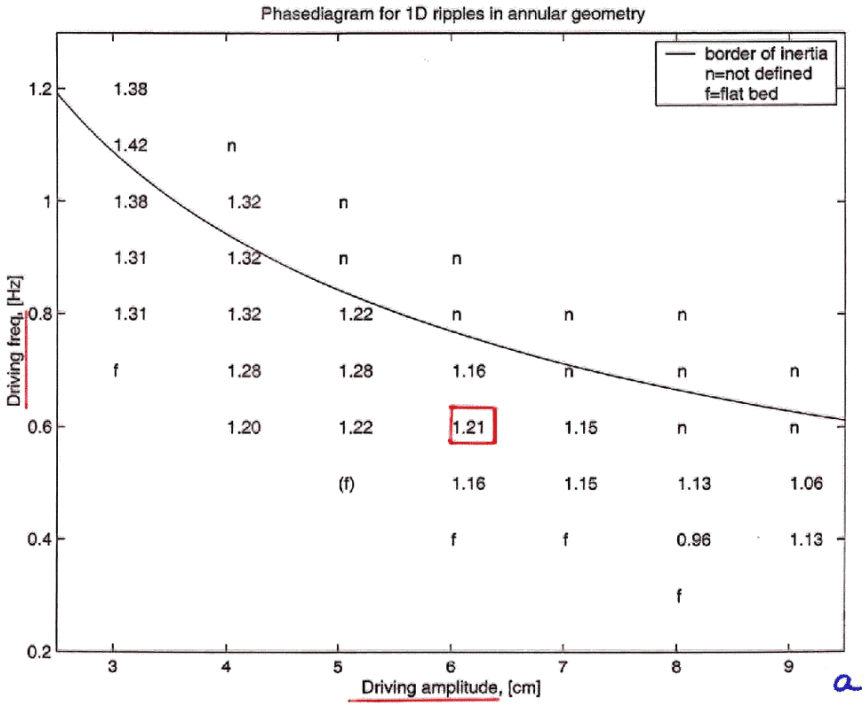

Figure 3: The phase diagram for scaled ripples (λ/a) made with flat bed as the initial condition. The time used for each measurement was four hours.

L. R. Sørdergaard, J. Udesen 4

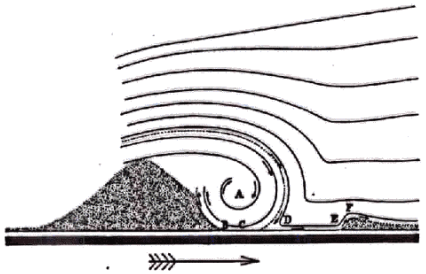

H. Ayrton (1910)

Fixed ripple $\lambda/a = 1.2$

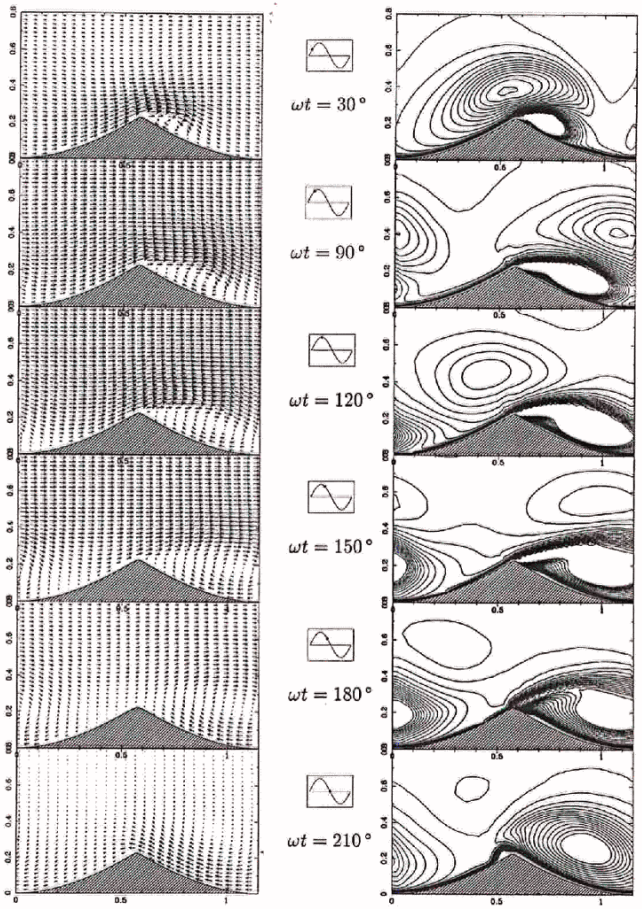

K. H. Andersen (1999)

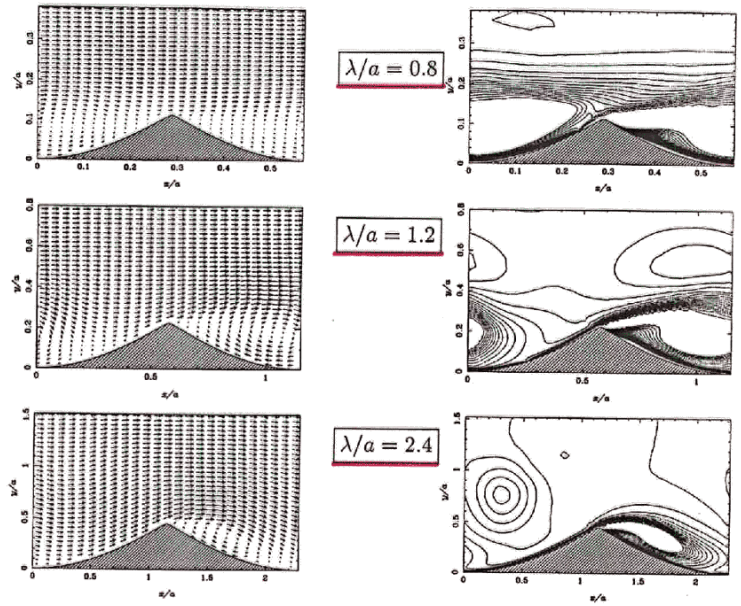

Figure 4.5: The flow at $\omega t = 120°$ for a the wave only situation, but with $\lambda/a = 0.6$ (top), $\lambda/a = 1.2$ (middle) and $\lambda/a = 2.4$ (bottom). The legend is as in figure 4.4.

K. H. Andersen (1999)

THE MASS TRANSFER MODEL

K.H. Andersen, M.-L. Chabanol, M. van Hecke: PRE **63**, 066308 (2001)

- Pattern evolves by mass transfer between fully developed ripples
- Mass transferred to ripple i from ripples $i \pm 1$ is a function $f(\lambda_i)$ of the size λ_i of ripple i

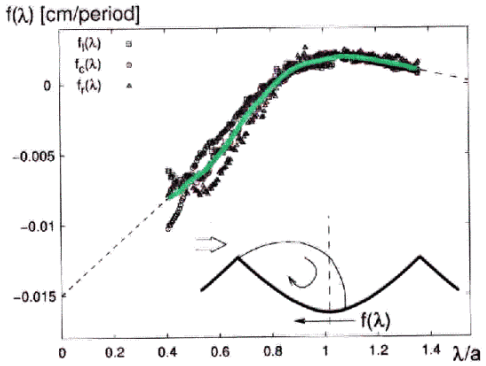

- Mass balance:

$$\dot{\lambda}_i = 2f(\lambda_i) - f(\lambda_{i+1}) - f(\lambda_{i-1})$$

$+$ relabeling when $\lambda_i \to 0$

$\Rightarrow$ uniform pattern $\lambda_i \equiv \bar{\lambda}$ is stable [unstable] when $f'(\bar{\lambda}) < 0$ [$f'(\bar{\lambda}) > 0$]

COARSENING DYNAMICS

Experiment (ripple crests)

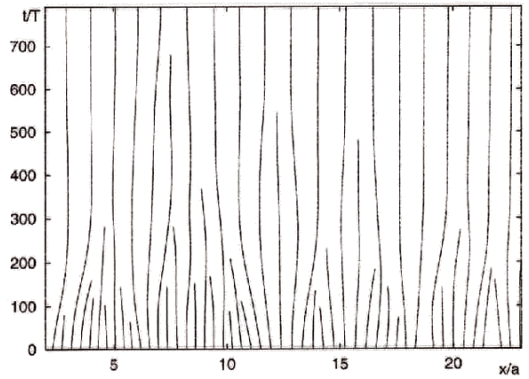

Simulation (ripple troughs)

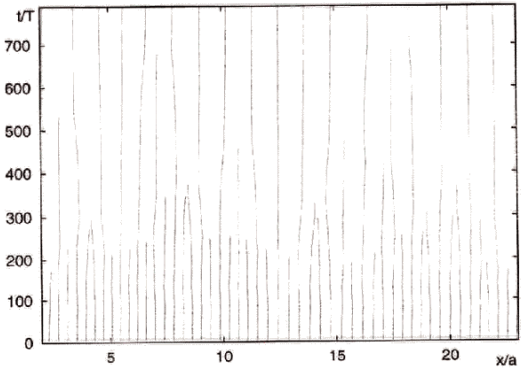

EXPERIMENTAL VALIDATION*

Ansatz:

$$\frac{d\lambda_i}{dt} = 2f_c(\lambda_i) - f_l(\lambda_{i-1}) - f_r(\lambda_{i+1})$$

Fit to time evolution using ACE algorithm yields:

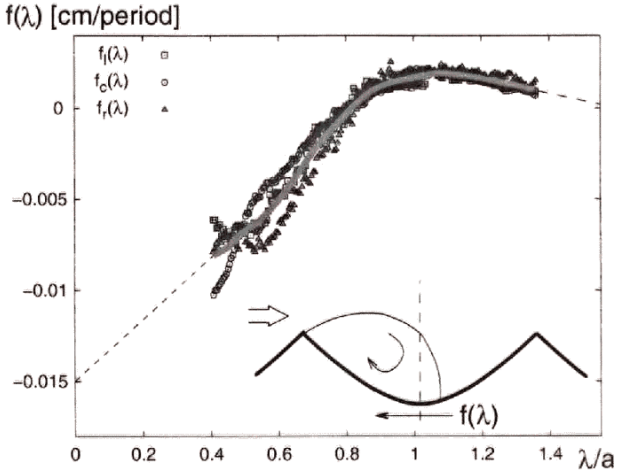

- Selected wavelength: $\tilde{\lambda}/a \doteq 1.25$
- Stable band: $1.13 \pm 0.03 \leq \lambda/a \leq 1.45 \pm 0.05$
- Model: $\lambda_c/a = 1.08$, $\tilde{\lambda}/a = 1.4$

*PRL 88, 234302 (2002)

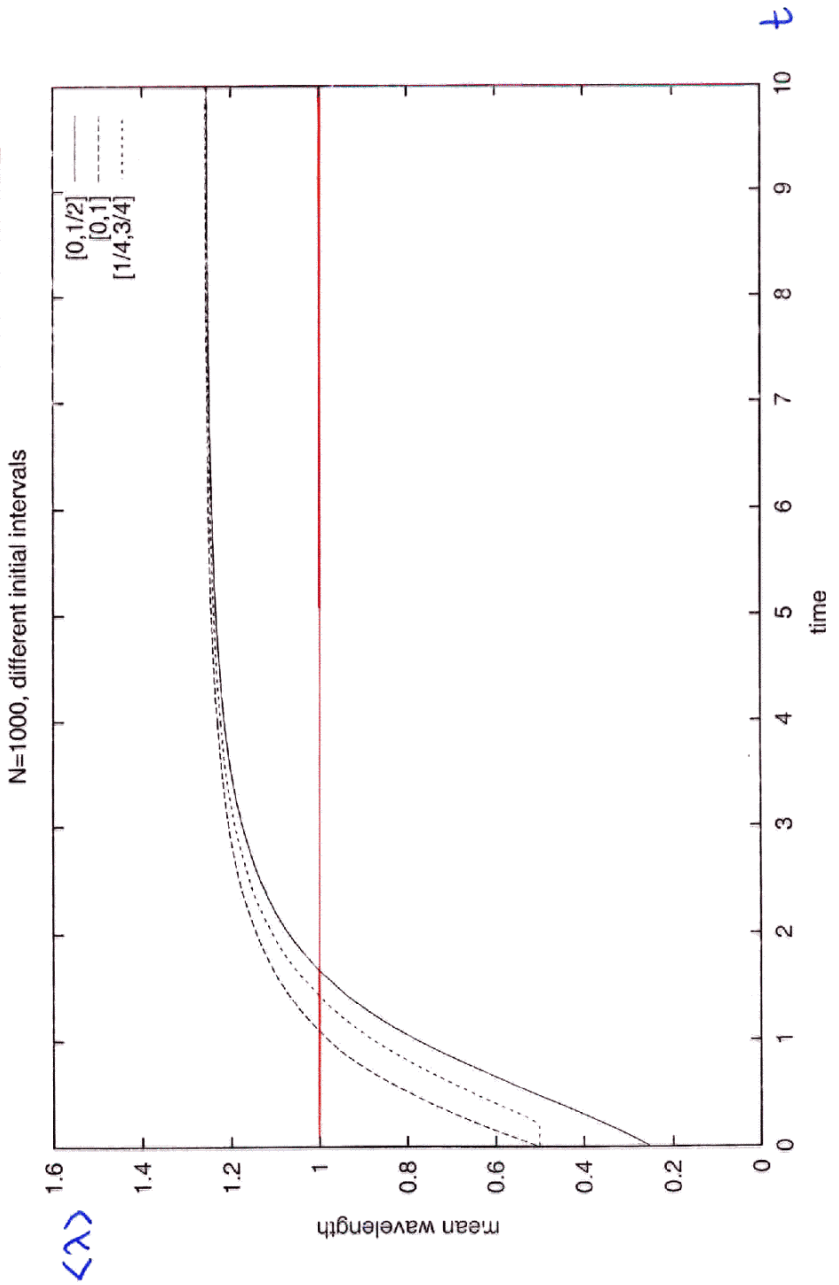

PARTICLE REPRESENTATION

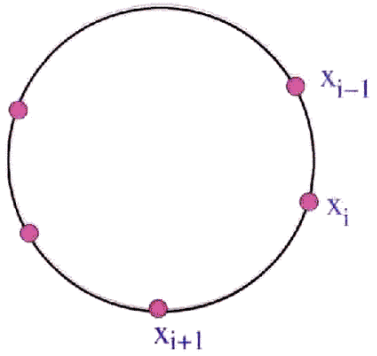

$$\lambda_i = x_{i+1} - x_i$$

$$\Rightarrow \quad \frac{dx_i}{dt} = -\frac{\partial V}{\partial x_i}, \quad V = \sum_i v(x_{i+1} - x_i)$$

$$v(x) = -\int_0^x d\lambda f(\lambda)$$ repulsive pair interaction

Conjecture:

Equilibrium wavelength λ^* is the minimum of V at fixed total length $N\lambda_i = L$

$\Rightarrow$ Maxwell construction for $f(\lambda)$:

$$\int_0^{\lambda^*} d\lambda \, f(\lambda) = \lambda^* \, f(\lambda^*)$$

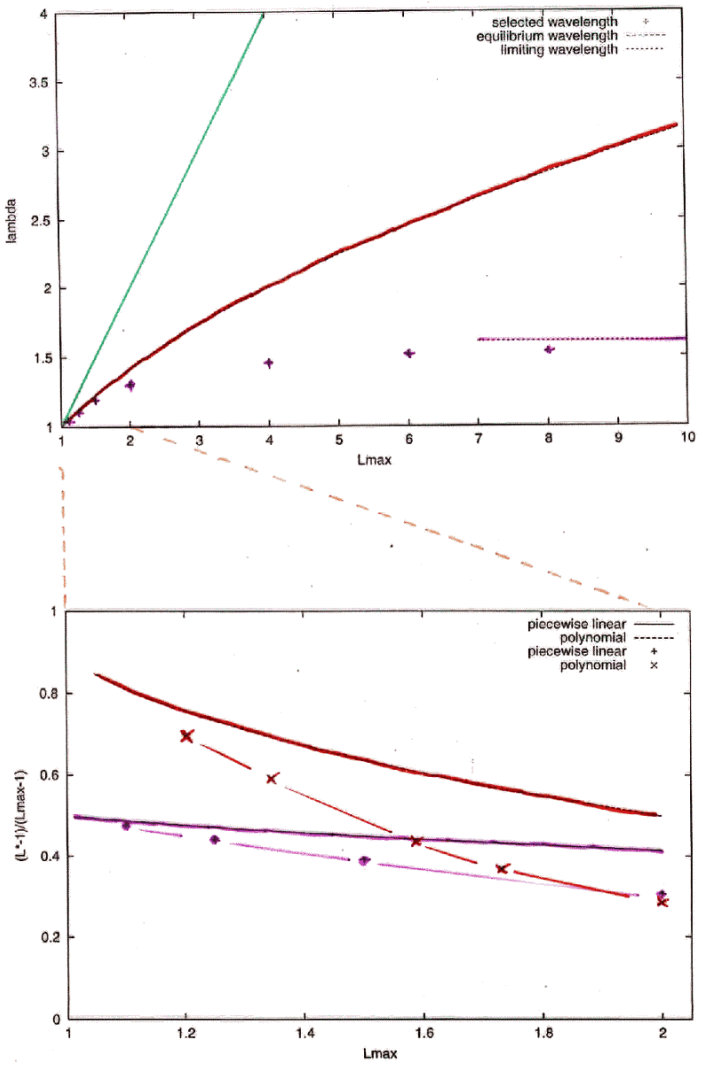

DOES IT WORK ?

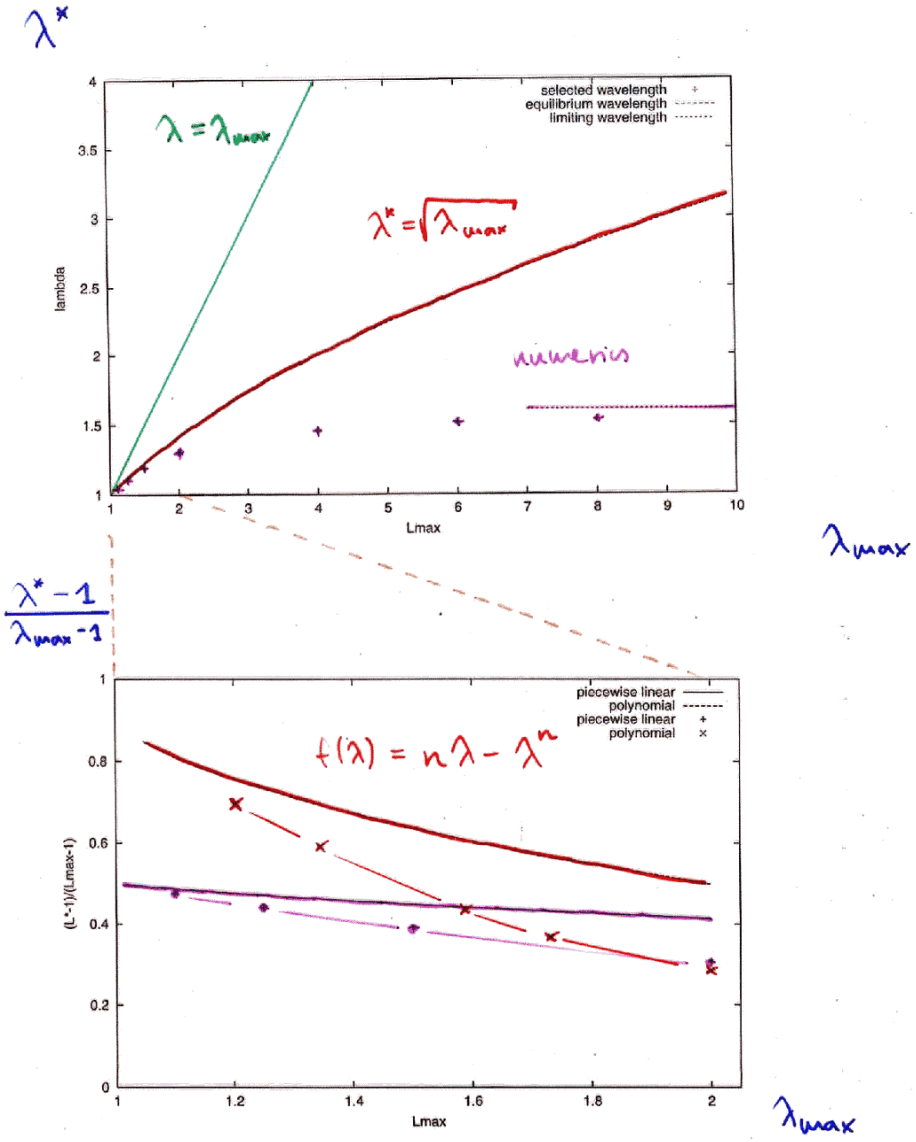

MONOTONIC TRANSFER FUNCTIONS

a simple choice: $\boxed{f(\lambda) = \lambda^\gamma}$

- $\gamma < 0$: Noise-induced coarsening

$$\langle\lambda\rangle \approx -\frac{1}{\gamma}\ln t$$

- $0 < \gamma < 1$: $\langle\lambda\rangle \sim t^{1/(1-\gamma)}$

- Mean field solution for $\gamma = 1$:

$$\frac{d\lambda}{dt} = \lambda - \langle\lambda\rangle(t)$$

$$\Rightarrow \lambda(\lambda_0, t) = [\lambda_0 - F(t)]e^t, \quad F(t) = \int_0^t ds\, e^{-s}\langle\lambda\rangle(s)$$

initial distribution $P_0(\lambda)$ evolves into

$$P_t(\lambda) = e^{-t}P_0(e^{-t}\lambda + F(t))$$

fraction of surviving ripples:

$$\int_0^\infty d\lambda\, P_t(\lambda) = \int_{F(t)}^\infty dx\, P_0(x) = \frac{\langle\lambda\rangle(0)}{\langle\lambda\rangle(t)}$$

Self-consistency condition:

$$\frac{dF}{dt} = \frac{e^{-t}\langle\lambda\rangle(0)}{P_o^c(F(t))}, \quad P_0^c(x) = \int_x^\infty dx'\, P_0(x')$$

$$\Rightarrow \quad \langle\lambda\rangle(t) \sim e^{\mu t}$$

with

$$\mu = \begin{cases} 1 & \text{exponential-like } P_0 \\ \frac{b}{b-1} & P_0 \sim \lambda^{-(b+1)} \\ \frac{a+1}{a+2} & P_0 \sim (\lambda_{\max} - \lambda)^a \end{cases}$$

$\Rightarrow$ **non-universal** with respect to P_0.

- Simulations for $\gamma = 1$ show **universality**:

$$P_t(\lambda) \to \langle\lambda\rangle^{-1} f(\lambda/\langle\lambda\rangle)$$

with $f(x) \sim e^{-cx}$, $\langle\lambda\rangle \sim e^t$.

THE WORM MODEL

B.T. Werner, D.T. Gillespie: PRL **71**, 3230 (1993)

- Wind ripples propagate at speed $v(\lambda) \sim 1/\lambda$

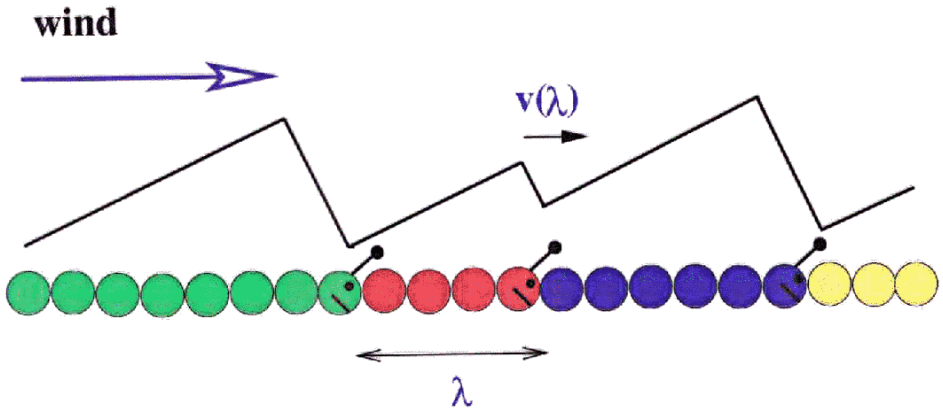

- Ripple i intrudes on ripple $i+1$ at rate $\sim 1/\lambda_i$

$$\Rightarrow \quad \dot{\lambda}_i = f(\lambda_i) - f(\lambda_{i-1}), \quad f'(\lambda) < 0$$

- Uniform pattern is linearly stable, but logarithmic coarsening $\bar{\lambda} \sim \ln t$ occurs due to stochastic merging

- Solution in "mean field" approximation

VOLUME 71, NUMBER 19 PHYSICAL REVIEW LETTERS 8 NOVEMBER 1993

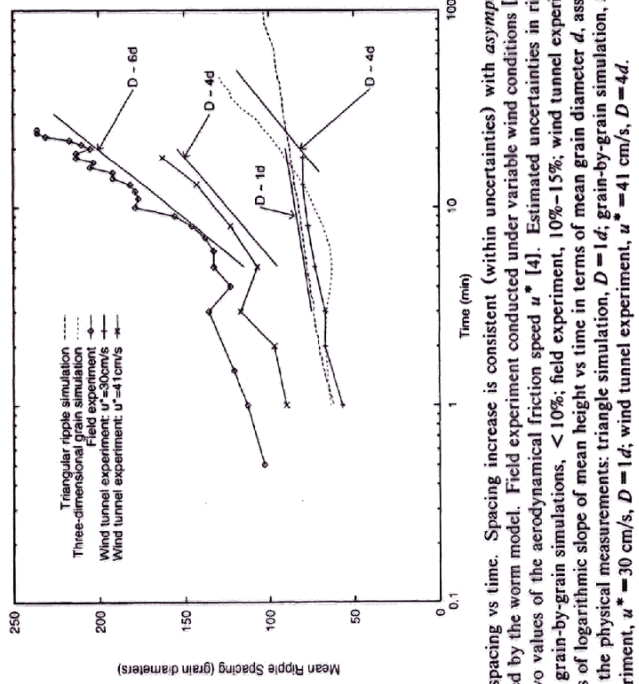

FIG. 4. Wind ripple spacing vs time. Spacing increase is consistent (within uncertainties) with *asymptotic* logarithmic dependence on time as predicted by the worm model. Field experiment conducted under variable wind conditions [2,5]; wind tunnel experiments performed with two values of the aerodynamical friction speed u^* [4]. Estimated uncertainties in ripple spacing: triangular ripple simulation, < 3%; grain-by-grain simulations, < 10%; field experiment, 10%–15%; wind tunnel experiments, uncertainties not provided. Inferred values of logarithmic slope of mean height vs time in terms of mean grain diameter d, assuming a ratio of spacing to ripple height of 10 for the physical measurements: triangle simulation, $D = 1d$; grain-by-grain simulation, $D = 4d$; field experiment, $D = 6d$; wind tunnel experiment, $u^* = 30$ cm/s, $D = 1d$; wind tunnel experiment, $u^* = 41$ cm/s, $D = 4d$.

GENERALIZED WORM MODELS

- Mass m_i at site i
- Jump $i \pm 1 \to i$ at rate $\Gamma(m_i) = m_i^\gamma$, $\gamma < 0$.
- Symmetric or asymmetric jumps
- Removal of empty sites & relabeling

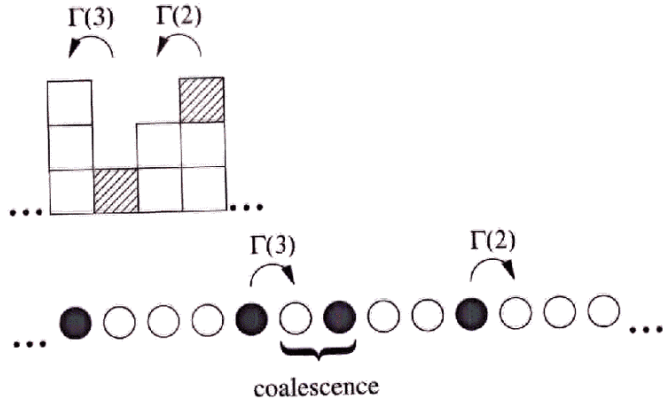

Related problems:

- zero range processes
- urn & backgammon models
- particle-particle coalescence with repulsive interactions

- Key observation: Separation of time scales between mass transfer and extinction

- Stationary product measures in the absence of extinctions:

$$P[\{m_i\}] = \prod_i p(m_i), \quad p(m) = p_0 \alpha^m [(m-1)!]^\gamma$$

$\gamma = 1$: Poisson distribution

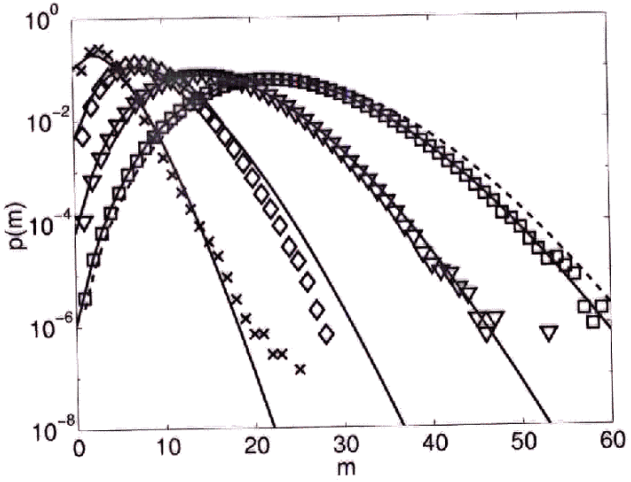

- Behavior for large m:

$$p(m) \sim e^{\gamma\langle m\rangle} \langle m\rangle^{-\gamma m-(1-\gamma)/2} [(m-1)!]^\gamma$$

$$\langle m^2\rangle - \langle m\rangle^2 \sim \langle m\rangle$$

- Derivation of the coarsening law:

$$\frac{d\langle m\rangle}{dt} \approx p(0)\langle m\rangle \sim e^{\gamma\langle m\rangle}\langle m\rangle^{-(1-\gamma)/2}$$

$$\Rightarrow \quad \langle m\rangle \approx -\frac{1}{\gamma} \ln t$$

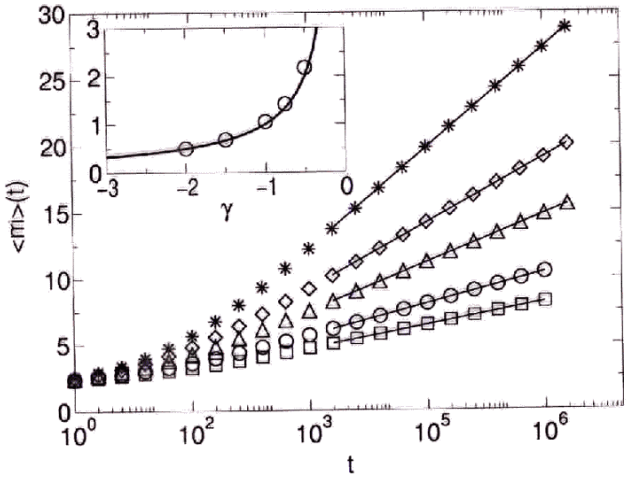

- Diffusive decay of correlations:

$$g(t) = \frac{\langle m_i m_{i+1}\rangle - \langle m\rangle^2}{\langle m\rangle^2} \sim t^{-1/2}$$

with logarithmic corrections

- KPZ asymptotics $g(t) \sim t^{-2/3}$ expected for asymmetric mass transfer and $t \gg (\ln t)^{3-\gamma}$

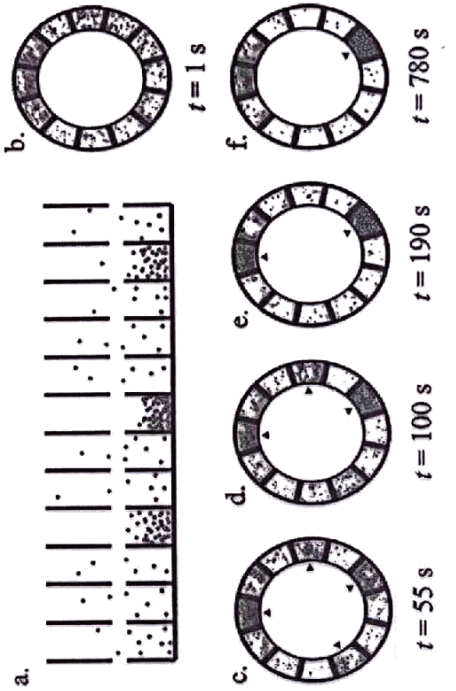

Figure 1. (a) A sketch of a vertically driven container partitioned into a cyclical array of 12 compartments connected by slits. Particles leaving the last compartment to the right enter the first from the left. (b)–(f) Snapshots (top view) of an experiment in 12 compartments initially filled uniformly with 480 steel beads of radius $r = 1.18$ mm. The driving strength is well within the clustering regime ($f = 40$ Hz, $a = 1$ mm). The compartments lie on a ring with inner diameter 80 mm and outer diameter 104 mm; they are connected by 5.0 mm high slits located 25 mm above the bottom and extending from the inner to the outer ring. The uniform distribution of particles at $t = 1$ s (b) quickly develops structures, of which the short lived transient with four clusters at $t = 55$ s is an example (c). At $t = 90$ s the system settles into a three-cluster state (d), which at $t = 180$ s coarsens into a two-cluster state (e), and on a much longer timescale (at $t = 770$ s) into the final state with only one cluster (f). The arrows in (b)–(f) mark the clusters.

D. van der Meer, K. van der Weele, D. Lohse

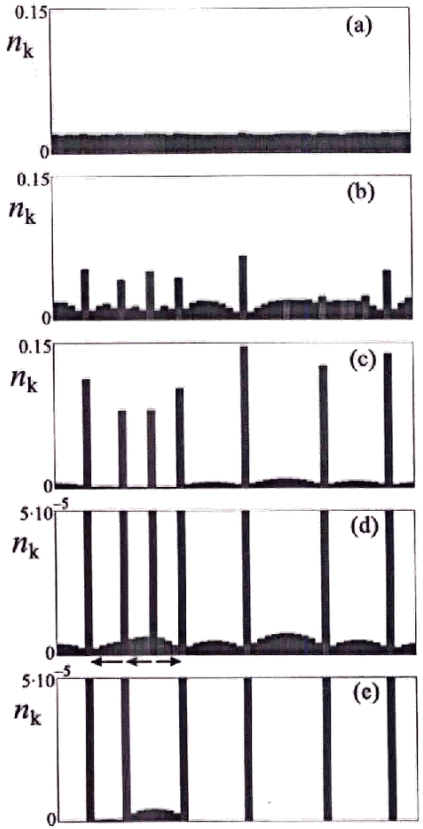

Figure 4. Five snapshots from the coarsening process within the flux model, with time measured in units of $C\sqrt{B}N^2$: (a) $t = 0$, initial state; (b) $t = 7.2 \times 10^2$, towards the end of the cluster formation stage; (c) $t = 2.1 \times 10^3$, depletion of the intermediate hilly pattern; (d) $t = 1.8 \times 10^6$, cluster-to-cluster transport, indicated by the arrows; (e) $t = 1.2 \times 10^8$, just after collapse of the third cluster from the left. The contents of this cluster have spread to its two direct neighbours, leaving a pronounced intermediate hill. Note the enlarged vertical scale in (d) and (e).

Rousseaux, Stegner, Westfreid

PHYSICAL REVIEW E 69, 031307 (2004)

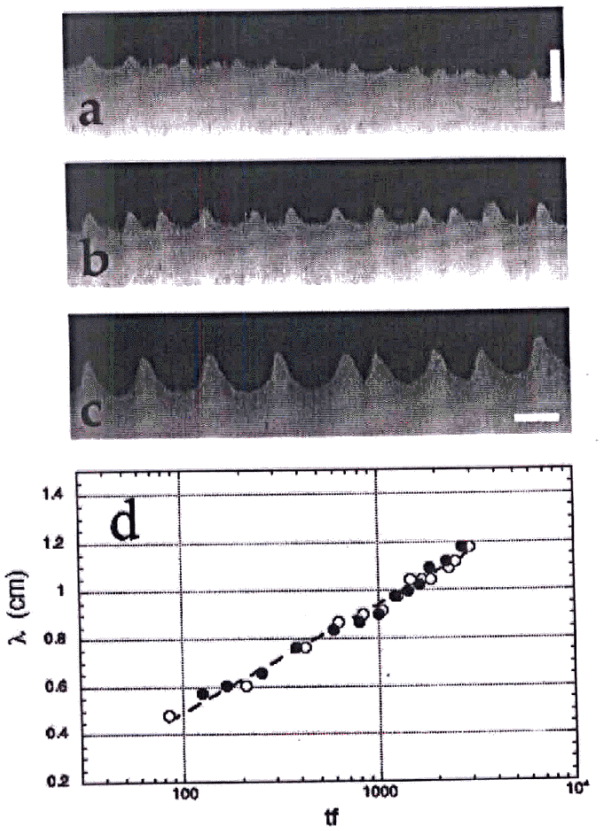

FIG. 8. (Color online) Morphological evolution of rolling-grain ripples during the coarsening process for $A = 2.4$ cm, $\delta = 670$ μm, $d = 110$ μm. Ripple shape after 120 (a), 600 (b), and 2700 (c) oscillations. The white rectangles give a vertical scale of 1 mm on picture (a) and a horizontal scale of 1 cm on picture (c). Corresponding evolution of the mean ripple wavelength with semilog axis (d). Open and full circles correspond to two different experiments.

CONTINUUM EQUATIONS ?

- required symmetries: conservation
  - $h \to h + c$
  - $x \to -x$
  - $h \not\to -h$ [1]
  - uphill current [2]
  - slope selection [3]

$$\Rightarrow \quad h_t + \overset{2}{h_{xx}} + h_{xxxx} + \overset{1}{(h_x^2)_{xx}} - \overset{3}{(h_x^3)_x} = 0$$

P. Politi (1998): Solutions coarsen as $\lambda \sim \ln t$

with noise: $\lambda \sim t^{1/4}$

- Conjecture: Conserved 1d equations show coarsening and/or unbounded steepening. Stable periodic solutions do not exist.

the tray back and forth sinusoidally. We started with completely regular patterns formed by pressing down a mould in the flat bed and then running the system (for a

the ripples become unstable to the formation of stationary 'pearls' in the troughs between the ripples, which again form a tilted pattern (Fig. 1c). Unlike bulging and

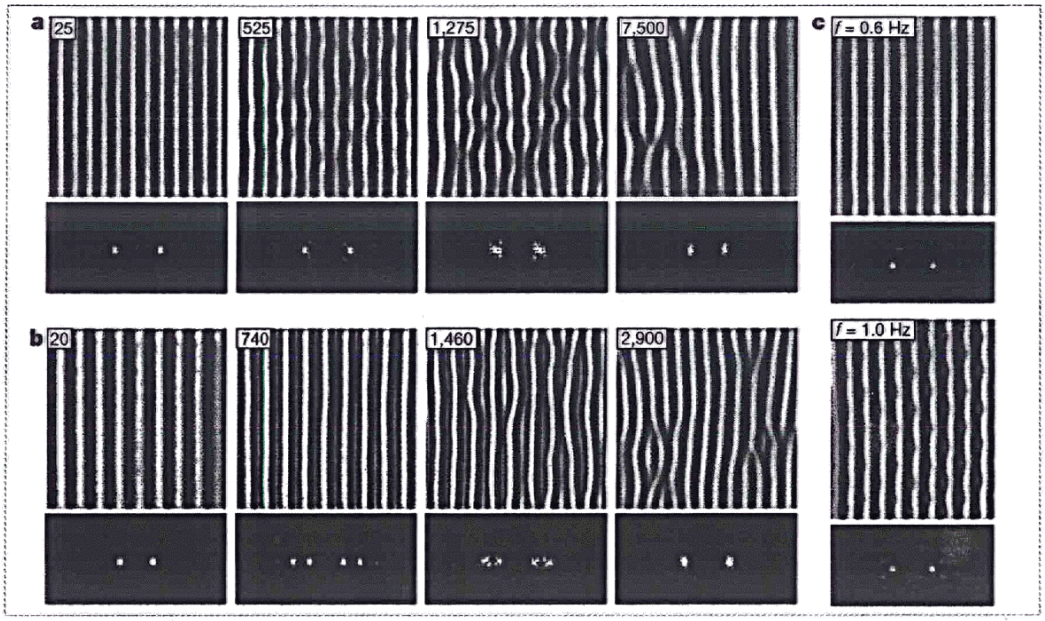

Figure 1 Patterns obtained by changing the driving parameters for a tray of sand oscillating in a water tank. **a, b,** Sequences of pictures from two experiments in which the amplitude of the drive was changed. The tray area in each is 53 cm × 53 cm; the light source was on the left and the sand tray was oscillated in the left–right direction; the camera was directly above the sand bed. Below each picture is shown the central region of the corresponding power spectrum, 2.32 m^{-1} × 1.16 m^{-1}. Numbers in the corners show the period at which the pictures were taken. For the top row (**a**), the initial wavelength was 4.2 cm, then the amplitude was 4.0 cm and the frequency 0.41

Bohr In
4. Scherer,
5. Stegner,
6. Cross, M
(1993).
7. Drazin,
Press, C

Palaeoa

Did
knu

All
T
be
howeve
DNA e
are mo
gorillas
analysis
joint,
African
commo
pose th
ciated
the bas
ble that
and th